Ain Shams Engineering Journal (2013) 4, 435–453

Ain Shams University

Ain Shams Engineering Journal

www.elsevier.com/locate/asej
www.sciencedirect.com

CIVIL ENGINEERING

Resistance of cold-formed steel sections to combined bending and web crippling

Mohamed Salah Al-Din Soliman, Anwar Badawy Badawy Abu-Sena *, Emad Emam Hassan Darwish, Mohamed Saeed Refaee Saleh

Faculty of Engineering (Shobra), Benha University, Egypt

Received 29 March 2012; revised 5 September 2012; accepted 5 October 2012
Available online 23 December 2012

KEYWORDS

Web crippling;
Interaction between web crippling and bending moment;
Cold-formed sections;
Finite element analysis;
Design codes

Abstract Web crippling is a common failure mode in cold formed sections. Interaction between bending and web crippling reduces the load carrying capacity and may control the design. In this research, numerical study on web crippling and interaction between bending and web crippling are performed considering the material and geometric nonlinearities. The study is performed on channel sections subjected to web crippling under interior one flange (IOF) loading conditions. Finite element models are verified against experimental tests, and then extended to predict the web crippling strength of the studied channel sections. FE is used to investigate the interaction between bending and web crippling in C-sections. FE results are employed to investigate the effect of different parameters on sections resistance. It was found that, the strengths predicted by design codes are generally inadequate for channels with a practical web slenderness range. Therefore, modifications were proposed to improve the strength predicted by codes.

1. Introduction

Cold formed steel sections are special sections which have high strength to weight ratio. The cold-formed steel C- and Z-sections are the most common sections used in building construction. These sections can be used as secondary beams (purlins) to support the light weight roof covering systems, also can be used as side girt, cassettes, etc. Many criteria govern the design of such sections such as, moment capacity, deflection, web shear resistance, web crippling, combined bending and shear and combined bending and web crippling.

Flexural capacity of a cold-formed steel beam in general is limited either by the effective section capacity or the lateral buckling capacity, especially when supported laterally at large intervals. On the other hand, web crippling of such beams depends on the cross section parameters (web slenderness ratio, web thickness and inside bend radius to thickness ratio) in addition to the material yield stress and the bearing length to web thickness ratio. Although, the webs of such sections have high depth to thickness ratio, using stiffeners under the concentrated loads is not practical in this type of construction.

* Corresponding author. Tel.: +20 111 067 6655.
E-mail address: abbadawy@yahoo.com (A.B. Badawy Abu-Sena).
Peer review under responsibility of Ain Shams University.

Production and hosting by Elsevier

2090-4479 © 2012 Ain Shams University. Production and hosting by Elsevier B.V. All rights reserved.
http://dx.doi.org/10.1016/j.asej.2012.10.006

List of symbols

C, C1: 20	non-dimensional coefficients
C	calibration coefficient
CH	web slenderness coefficient
CN	bearing length coefficient
CP	correction factor
CR	inside bend radius coefficient
$C\theta$	non-dimensional coefficient;
d, D	overall web depth
h, hw	flat web depth
E	Young's modulus, 21,000 N/mm^2
F	extreme compression or tension fiber at design stress
$F_{0.2}$	proof stress
F_m	mean value of fabrication factor
F_u	ultimate strength of steel
F_W	concentrated web load or reaction (kN)
F_y	design yield stress
Fyc	rounded corner yield stress
k	web crippling coefficient
L	specimen total length
M	bending moment at the point of application the concentrated load P
m	conversion coefficient
$\overline{M}$, M, M_u	the corresponding ultimate bending moment at the point of the applied ultimate concentrated load or reaction, $\overline{P}$ or P_u respectively
M_C	moment capacity determined as Se F
M_m	mean value of material factor
M_{nxo}	nominal flexural strength about the x-axis
N	bearing load length
n	number of tests or models
$\overline{P}$,, P, P_u	the ultimate concentrated load or reaction in the presence of bending moment.
PC-Exp	ultimate test load accompanied by bending moment
PFE	predicted finite element load
P_m	mean value of professional factor for tested component
P_n	nominal ultimate web crippling load or reaction per web
Pult	ultimate crippling load (kN)
P_w	concentrated load resistance of single web
py	design strength in N/mm^2
R	inside bend radius
R_n	average value of all test results
Se	elastic section modulus of effective section
t	web thickness
β	target reliability index
θ	angle between plan of web and plan of bearing surface
Φ_b	resistance factor for bending
Φ_w	resistance factor for web crippling

Therefore, the web crippling is a governing criterion that may control the design.

Theoretical study of web crippling is very complicated because many factors should be considered. These factors are the non-uniform stress distribution under the applied load, the local yielding at the loaded area, the bending due to eccentric loading, elastic and inelastic behavior of the web element, the different web flange restraint and the initial imperfections of the web element, Yu [16]. That is why most of researches on web crippling and combined bending and web crippling are experimental. Recently, with the progress achieved in the field of computer programming, the numerical analysis using an approved finite element tool is a good alternative to the experimental work.

Interaction between bending and web crippling is a common behavior in cold formed steel construction and will be also studied carefully in light of the continuous modifications of web crippling strength prediction. The adequacy of the web crippling and bending interactive formulae of the design codes will be also investigated.

This research is focused on the behavior of cold formed steel C-sections subjected to web crippling and interaction of bending and web crippling under interior one flange loading condition as indicated Fig. 1.

The parameters range of the studied channel dimensions are: web heights (D = 100, 150, 200 and 250 mm); web thicknesses (t = 2 and 3 mm); inside bend radiuses (R = 6 and 9 mm) and constant flange width (b = 50 mm). The bearing lengths are (N = 25, 50 and 75 mm) in addition to using two different steel yield stresses (F_y = 240 and 360 N/mm^2).

In addition to the mentioned parameters range, two different span lengths are used (L = 1000 and 2000 mms) for studying the interaction of bending and web crippling strengths. In this study four different design specifications are included in comparisons, the Australian/New Zealand Standard (AS/NZS-4600), British Standard (BS:5950-5), Egyptian Code of Practice (ECP-LRFD) and North American Specification (NAS).

2. Literature review

Due to its complexity, most researches on web crippling are mainly experimental and numerical. In this section, reviews of the experimental and numerical researches on web crippling and combined bending and web crippling are presented.

Experimental researches on web crippling of cold formed steel sections started in 1939 at Cornell University. Based on the results of these researches, the first American Iron and Steel Institute design code was published (AISI-1946). The first Canadian code for cold formed steel design was presented in 1963, while the first European code was published in 1970s. Experimental researches continued and the design provisions of AISI were updated in 1956, 1960, 1962, 1968, 1980, 1986, 1991 and 1996, while the Canadian code was updated in 1974, 1984, 1989 and 1994 (S136-94) [7]

In most of the current design codes, there are four different load cases considered in design against web crippling. The difference between the four load cases is based on the applied load location and whether the applied loads acting on both flanges or not. The different four load cases are shown in Fig. 2.

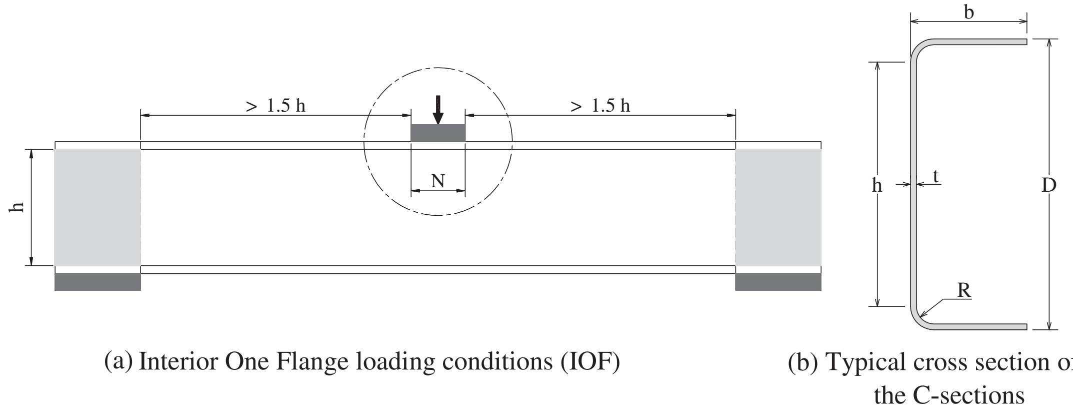

Figure 1 Geometry, loading and supporting conditions.

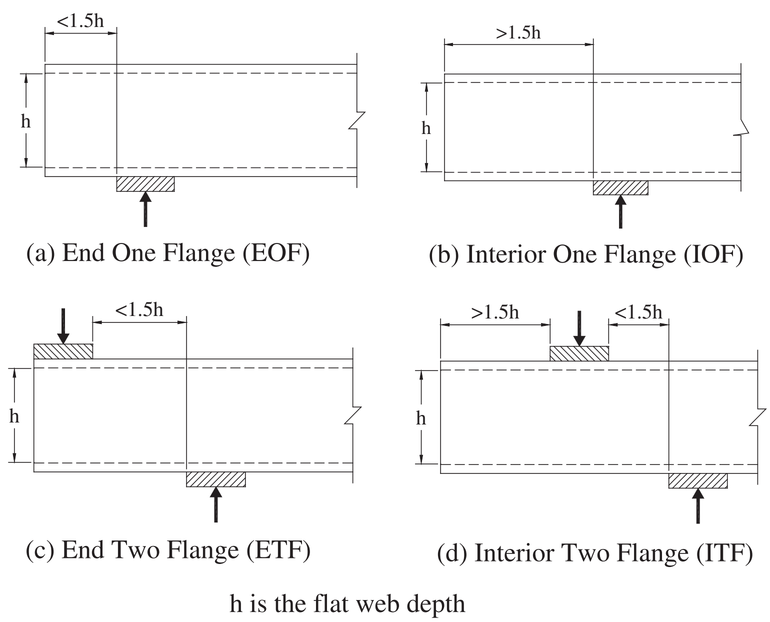

Figure 2 One and two flange loading conditions.

In 1993, Parabakaran [9] carried out an extensive statistical study on web crippling of cold formed sections at Waterloo University. Based on the available experimental results from the literature, Parabakaran proposed a unified equation for web crippling strength with different coefficients. For I-sections and shapes having single un-reinforced webs, the unified equation was limited to $(h/t) \leqslant 200$, $(N/t) \leqslant 200$, $(N/h) \leqslant 1$ and $(R/t) \leqslant 4$. While the limitations for multi-web decks were $(h/t) \leqslant 200$, $(N/t) \leqslant 200$, $(N/h) \leqslant 2$ and $(R/t) \leqslant 10$.

Beshara and Schuster [3,4] performed a statistical study on the web crippling of cold formed steel sections. They collected the web crippling data existing at the university of Waterloo in addition to carrying out 72 tests on C and Z specimens not included before within the collected data. The objective of the study was improving the coefficient used in Parabakaran unified design equation. The modified coefficients were adopted in the North American Specification (NAS-2001). It was observed that, the final coefficients of C-sections subjected to IOF loading conditions were based on 32 test results for stiffened C-sections and 20 test results for un-stiffened sections.

Young and Hancock [12–15] carried out a series of tests on cold formed un-lipped having thickness up to 6 mm and maximum web slenderness ratio of 45 steel channels subjected to web crippling under four different load cases (EOF, IOF, ETF and ITF). The test strengths were compared to the design strengths calculated using AISI 1996, AS/NZS-4600 and NAS Specifications. It was concluded that the predicted web crippling strengths by AISI 1996 and AS/NZS-4600 specifications are generally un-conservative for un-lipped channels under the four loading conditions. On the other hand the NAS specification was conservative for ETF and ITF loading.

In 2006, Ren et al. [10,11] carried out a series of nonlinear finite element models based on a series of laboratory tests on cold formed steel channels subjected to web crippling under both, end one flange (EOF) and interior one flange (IOF) loading. The finite element models included geometric and material nonlinearities. The developed finite element models were verified against test results in terms of the ultimate loads, the load versus web deformation curves and the web crippling failure modes. The web crippling strengths obtained from finite element analyses were compared with the predicted design strengths using the North American Specification (NAS-2001). It was concluded that the design strengths are generally un-conservative for channels having web slenderness (h/t) ranged from 7.8 to 108.5 and subjected to end one flange or interior one flange loading conditions.

3. Current design specefications

3.1. North American specification

3.1.1. Web crippling strength

NAS specification [8], gives unified design expression (Eq. (1)) for calculating the web crippling strength for different cross sections. The unified design expression includes four different coefficients depending on the cross-section shape, applied load position, type of loading, whether the flanges are stiffened or not and fastened to the support or not. It is valid for I-, C-, Z-, hat and multi web deck sections.

$$P_n = C \cdot t^2 \cdot F_y \cdot \sin\theta \left(1 - CR\sqrt{\frac{R}{t}}\right) \cdot \left(1 + CN\sqrt{\frac{N}{t}}\right) \cdot \left(1 - Ch\sqrt{\frac{h}{t}}\right) \quad (1)$$

According to NAS, P_n represents the nominal strength for bearing load or reaction for one solid web connecting top and bottom flanges. For sections consisting of two or more webs, P_n shall be calculated for each individual sheet and the results are added to obtain the nominal strength for the full section. Coefficients of Eq. (1) are tabulated in NAS [8].

3.1.2. Interaction of bending and web crippling

According to NAS [8], for shapes having single un-reinforced webs and subjected to a combination of bending and concentrated load or reaction, the following requirements shall be satisfied in design According to the load and resistance factor design (LRFD) method:

$$\overline{P} \leqslant \Phi_w P_n \quad (2.a)$$

$$\overline{M} \leqslant \Phi_b M_{\text{nxo}} \quad (2.b)$$

$$0.91\left(\frac{\overline{P}}{P_n}\right) + \left(\frac{\overline{M}}{M_{\text{nxo}}}\right) \leqslant 1.33\phi \quad (2.c)$$

3.2. Egyptian code ECP-LRFD

3.2.1. Web crippling strength

According to ECP-LRFD [6], the nominal web crippling strength for shapes having single thickness webs under interior one loading conditions is calculated according to Eq. (3), Which is applicable to beams with $h/t \leqslant 200$ and $R/t \leqslant 6$.

$$P_n = t^2 k C_1 C_2 C_{12} C_{15} C_{19} \times 10^{-4} \quad (3)$$

3.2.2. Interaction of bending and web crippling

For shapes having single un-reinforced webs subjected to a combination of bending and web crippling, the following interaction equation should be satisfied when using LRFD method:

$$1.07\left(\frac{Pu}{\phi_W P_n}\right) + \left(\frac{Mu}{\phi_b M_{nxo}}\right) \leqslant 1.42 \quad (4)$$

3.3. British Standard BS 5950-5

3.3.1. Web crippling strength

The web crippling resistance of beams having single webs, according to BS 5950-5 [5], is calculated using the following equation:

$$P_w = t2kC1C2C12\{3350 - 4.6(D/t)\} \times \{1 + 0.007(N/t)\} \quad (5)$$

3.3.2. Interaction of bending and web crippling

According to BS 5950-5 [5], flat webs of sections having single thickness webs subjected to a combination of bending and web crippling should be designed to satisfy the following requirements at the limit state:

$$F_W \leqslant P_W \quad (6.a)$$

$$M \leqslant M_C \quad (6.b)$$

$$1.1\left(\frac{F_w}{P_w}\right) + \left(\frac{M}{MC}\right) \leqslant 1.50 \quad (6.c)$$

3.4. Australian/New Zealand Standard AS/NZS-4600

3.4.1. Web crippling strength

The Australian/New Zealand Standard for Cold-Formed Steel Structures AS/NZS [2], gives design equations that are similar to the AISI-1996 equations, but with modulus of elasticity E = 200000 N/mm^2.

$$P_n = t^2 k C_1 C_2 C_9 C_\theta \ [538 - 0.74(h/t)][1 + 0.007(N/t)] \quad (7)$$

When $N/t > 60$, the factor [1 + 0.007 (N/t)] may be increased to [0.75 + 0.011 (N/t)]

3.4.2. Interaction of bending and web crippling

According to AS/NZS 4600, for shapes having single un-reinforced webs subjected to a combination of bending and web crippling, the following interaction equation should be satisfied when using LRFD method:

$$1.07\left(\frac{Pu}{\phi_W P_n}\right) + \left(\frac{M_u}{\phi_b M_{\text{nxo}}}\right) \leqslant 1.42 \quad (8)$$

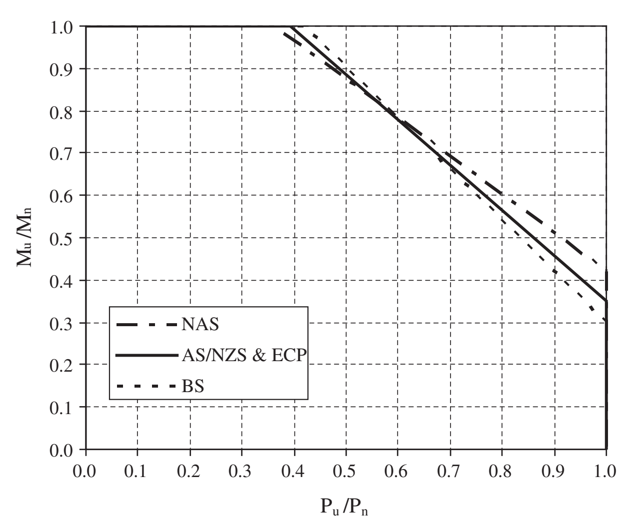

Figure 3 Different interaction design equations.

Fig. 3 shows a comparison between the interaction equations utilized by the different codes of practice.

4. Finite element modeling and verification

The finite element analysis in this research was carried out using the nonlinear finite element program **ANSYS 5.4** [1] to simulate the tested cold-formed steel channels. The measured cross-section dimensions, material properties and boundary conditions from tests were used in developing the FE models. The finite element models were verified against tests carried out by Young and Hancock [12,13] and then used for an extensive parametric study for different channel dimensions. The same test arrangement used by Young and Hancock [12] as shown in Fig. 4 was used in the finite element models. Each modeled specimen was divided into three parts along its length (L); supporting areas, bearing load area (N) and the distance in-between. In tests, each specimen was composed of a pair of channels to provide symmetric load conditions. In models, one quarter of the tested specimens was simulated making use of the symmetry that provided in tests.

4.1. Model arrangement

Each modeled specimen was divided into three parts along its length (L); supporting areas, bearing load area (N) and the distance in-between. In tests, each specimen was composed of a pair of channels to provide symmetric load conditions. In models, one quarter of the tested specimens was simulated making use of the symmetry that provided in tests. Fig. 5 shows the model arrangement utilized for different cases.

4.2. Element types and mesh

A shell element (Shell43 in ANSYS program) was used to model the channel specimens and the rigid bearing plates. This is a 4-node shell element with six degree of freedoms at each node. The Shell43 element is capable of describing plasticity, large deflections and large strains. 3D structural bar element (Link10) was utilized to model the contact between the rigid bearing plates and channels flange. The Link10 element has three degrees of freedom at each node: translations in x, y and z-directions. The Link10 element has options to resist tension-only or compression-only. With the option of compression-only, the stiffness is null in tension. No bending stiffness

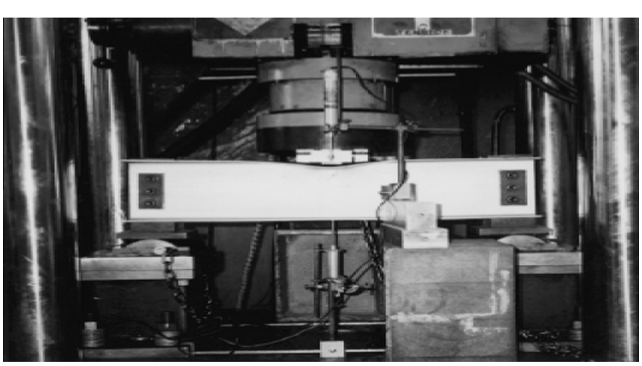

Figure 4 Interior-One-Flange (IOF) test setup [12].

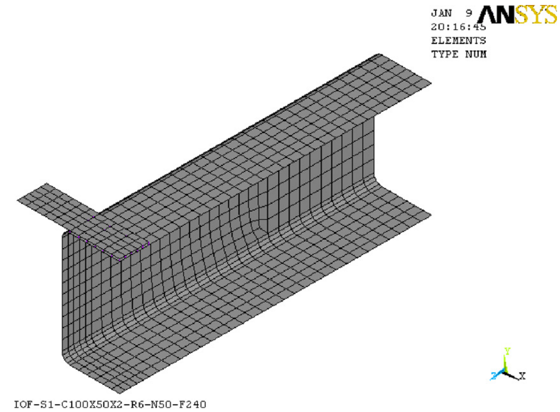

(a) Web crippling model "S1-C100×50×2-R6-N50-F240"

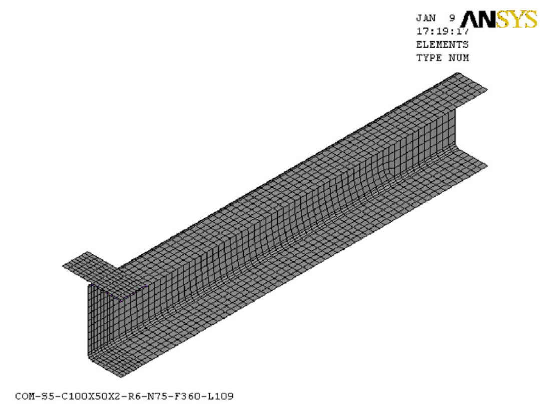

(b) Combined bending and web crippling model "S5-C100×50×2-R6-N75-F360- L109"

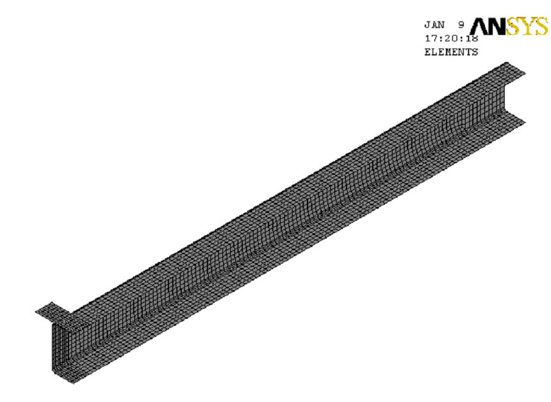

(c) Combined bending and web crippling model "S5-C100×50×2-R6-N75-F360- L209"

Figure 5 Finite element model arrangement for different cases.

is included in either the tension-only or the compression-only options. Link10 has the capabilities of large deflection.

The finite element mesh in the models was investigated by varying the size of elements. In the flanges and web, the size of the elements was 4.5 mm × 9 mm (length by width) in the part where the bearing load was applied and about

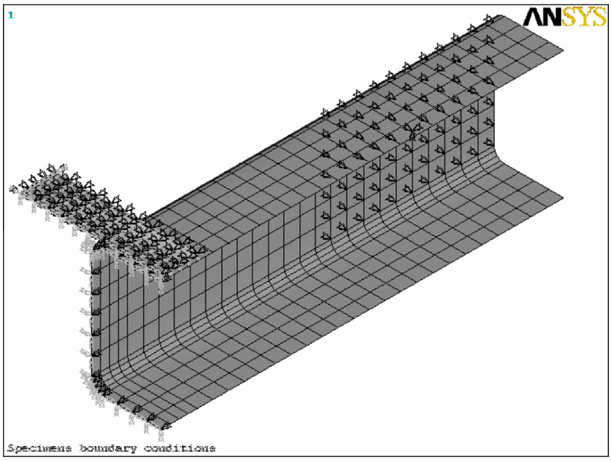

Figure 6 Model boundary and symmetry conditions.

9 mm × 9 mm elsewhere. A finer mesh was used in corners due to its importance in transferring the load from flange to web. The typical finite element models of cold formed channels subjected to combined bending and web crippling are shown in Fig. 5.

4.3. Boundary and symmetry conditions

Due to the symmetry conditions in test setup, it is sufficient to model only one quarter of the tested specimen. The symmetry conditions were applied at the mid span of the specimen cross section and at the middle of the bearing plate as shown in Fig. 6. Lateral and longitudinal displacements of the bearing plate were prevented but the vertical movement was allowed.

The test loading was simulated as a surface load distributed on rigid bearing plate supported by very stiff compression elements rested on the channel flange. The bearing plate was allowed to move vertically downward (y-direction) in rigid manner by means of vertical displacement constrain. The predicted ultimate load of this model was the closest to the predicted test load.

4.4. Material properties

The same material properties used in tests [12] were adopted for verification of FE models, and also applied for the performed parametric study. The strain hardening effect on the channel rounded corners due to the cold-forming were considered by using two different materials, one for the flat parts and the other for the rounded parts. The two materials had different yield stress and the same modulus of elasticity $E = 200{,}000\ \text{N/mm}^2$ and Poisson's ratio $\mu = 0.3$. The proof stress ($F_{0.2}$) from tests was used as a yield stress (F_y) for the flat parts and a modified yield stress (F_{yc}) was used for the rounded corner elements. The modified yield stress (F_{yc}) was calculated according to NAS specifications as follows.

$$\frac{F_{yc}}{F_y} = \frac{B_c}{\left(\frac{R}{t}\right)^m} \tag{9.a}$$

$$B_c = 3.69\frac{F_u}{F_y} - 0.819\left(\frac{F_u}{F_y}\right)^2 - 1.79 \tag{9.b}$$

$$m = 0.192\frac{F_u}{F_y} - 0.068 \tag{9. c}$$

Material nonlinearity through FE analysis models was achieved using the option of bilinear isotropic hardening. This option is often preferred for large strain analyses. Data needed

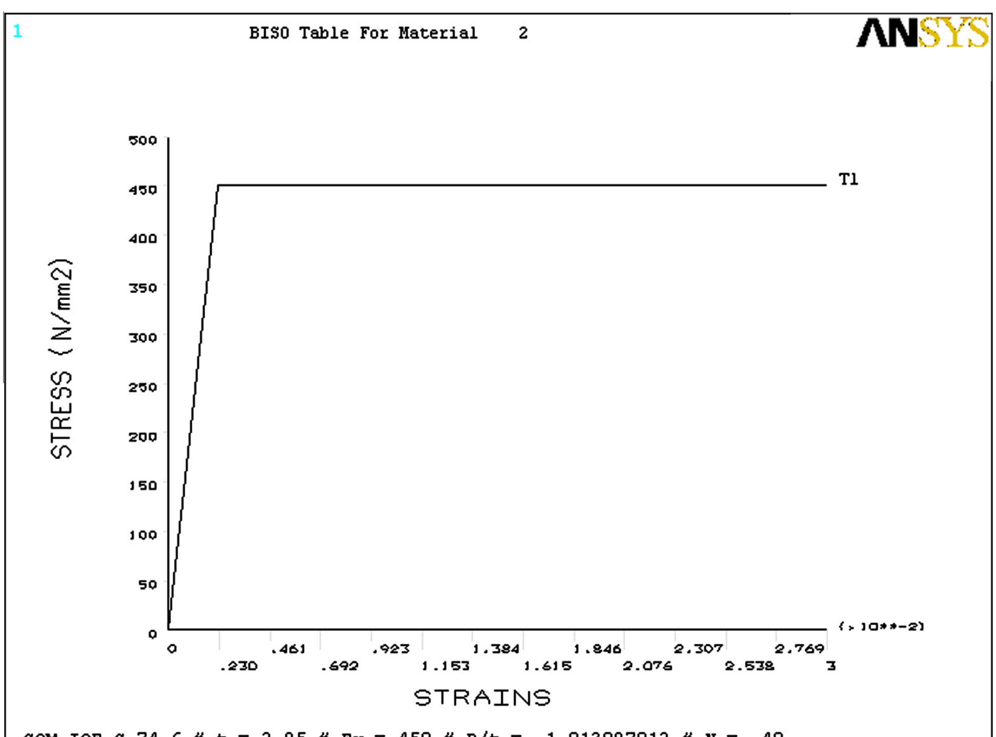

Figure 7 Bi-linear idealization of the stress-strain relation used in FE analysis.

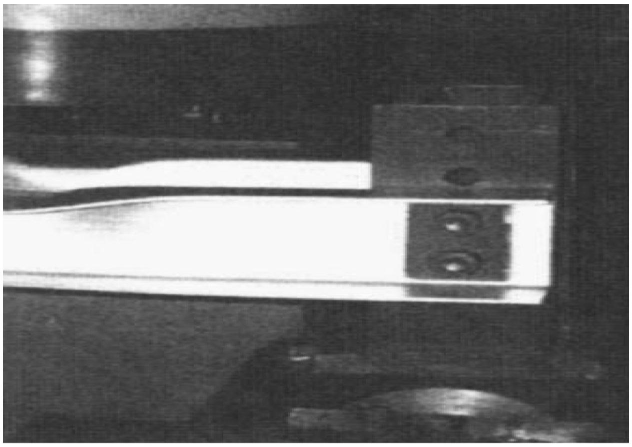

(a) Tested specimen at failure,

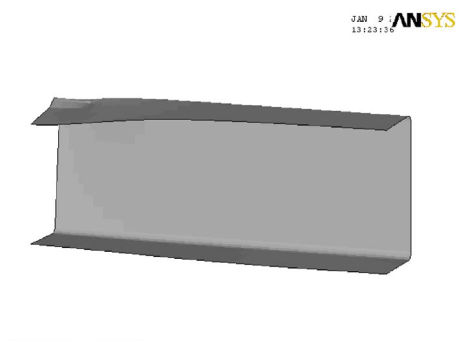

(b) Finite element model at failure

Figure 8 Comparison between test and FE deformed shaes.

for applying this option are young's modulus (*E*) and material yield stress as shown in Fig. 7.

4.5. Finite element verifications

One model was developed to simulate the IOF loading tests for predicting web crippling load and the same model arrangement but with fixed lengths was utilized for interaction of bending and web crippling of cold formed steel channels. The FE models were verified against experimental results obtained by Young and Hancock [12] in terms of web deformed shape and ultimate web crippling load.

Fig. 8 shows a comparison between the deformed shape obtained from test and from the finite element analysis performed using ANSYS5.4.

Fig. 9 shows a comparison between the web crippling strength obtained from tests and that obtained using ANSYS5.4. Fig. 10 shows a similar comparison for the combined bending and web crippling loads.

5. Finite element analysis

The analysis results of 192 finite element models (96-web crippling models and 96-bending and web crippling models) carried out on cold formed steel channels subjected to web crippling under (IOF) loading case are presented. The influence of cross section parameters on web crippling strength is discussed. The finite element strengths are compared with the design strengths predicted by AS/NZS, BS-5950, ECP and NAS specifications. The comparisons include both web crippling and interaction of bending and web crippling models. New web crippling coefficients are calibrated and proposed for the ECP and NAS unified web crippling design equation. Also, modified interaction equation is suggested for both codes.

Eight different channel sections (S1–S8) of different dimensions and material properties have been utilized for performing the finite element analysis. Dimensions and material properties of the eight sections are listed in Table 1.

5.1. Analysis results of web crippling models

The modeled channels were labeled such that the series number, the cross section type, the total web depth, the total flange width, the cross section thickness, the inside bend radius, the bearing load length and the material yield strength could be identified. For example, specimen label "S7-C100 × 50 × 2-R9-N50-F360" defines the following:

1. The first two characters indicate that the specimen belongs to a series "S7".

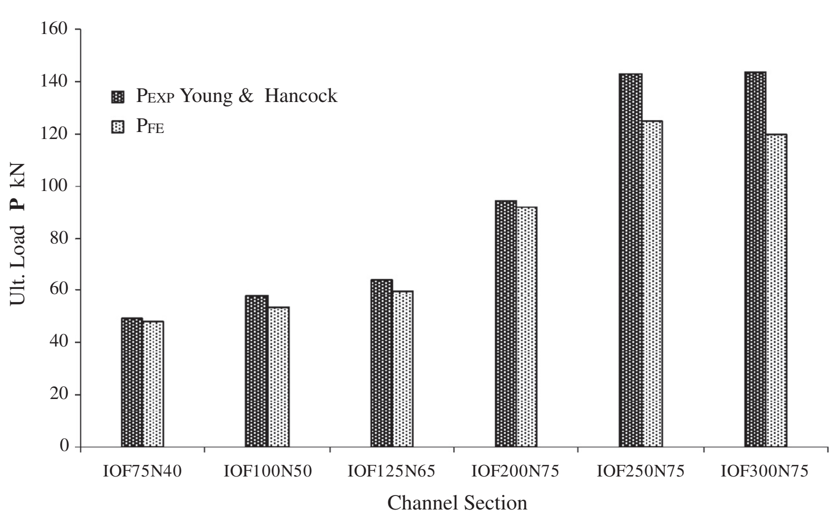

Figure 9 Experimental web crippling loads versus finite element ultimate loads.

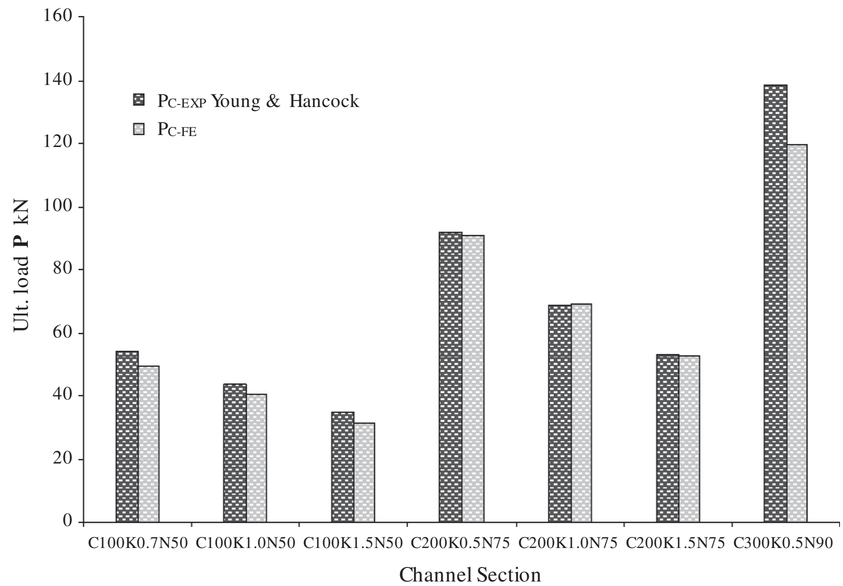

Figure 10 Experimental combined bending and web crippling loads versus finite element ultimate loads.

Table 1 Material properties and dimensions of channel sections.

Series name	Thick, t (mm)	Radius, R (mm)	Yield stress, F_y (N/mm^2)	Ultimate stress, F_u (N/mm^2)
S1	2	6	240	360
S2	3	6	240	360
S3	2	9	240	360
S4	3	9	240	360
S5	2	6	360	520
S6	3	6	360	520
S7	2	9	360	520
S8	3	9	360	520

2. The next four characters indicate that a Channel cross section of total web depth, D = 100 mm
3. The next two numbers indicate that the channel flange width, b = 50 mm.
4. The next number indicates that the channel thickness, t = 2 mm.
5. The next two characters indicate that the inside bend radius, R = 9 mm.
6. The next three characters indicate that the length of bearing load, N = 50 mm.
7. The last four characters indicate that the material yield stress, F_y = 360 N/mm^2.

Fig. 11 shows samples of Von Mises stress distributions and deformed shapes for two different web crippling specimens at the ultimate load. For web crippling models, the ultimate load was defined as the load accompanied with yielding of the top web- flange intersection along the complete bearing load length. For interaction between bending and web crippling models, the ultimate load was that accompanied with yielding of either the top or bottom web-flange intersection along the bearing load length.

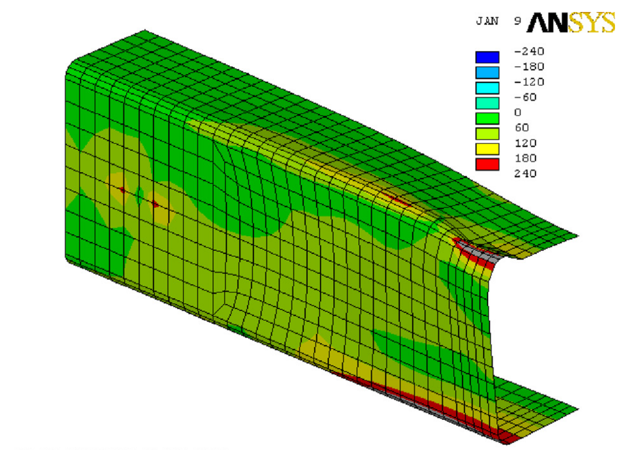

(a) IOF: S1-C100x50x2-R6-N50-F240

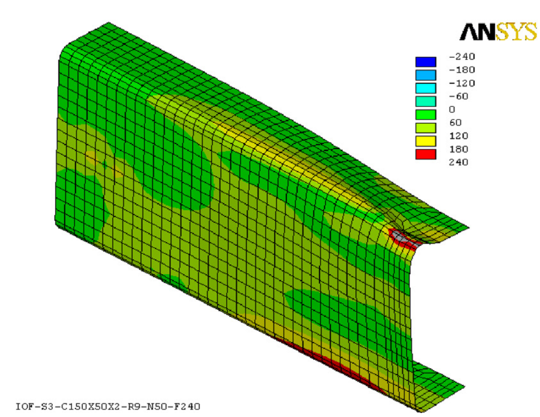

(b) IOF: S3-C150x50x2-R9-N50-F240

Figure 11 Von Mises stresses distribution and deformed shapes for two web crippling models.

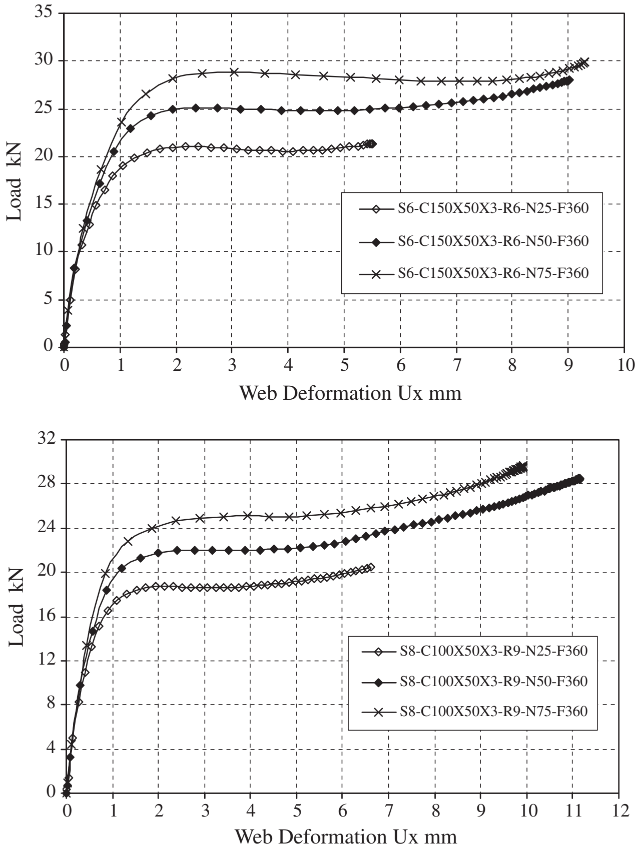

Figure 12 Load versus web deformations for different web crippling models.

Fig. 12 shows samples of load versus web deformation curves for different web crippling models. In most models it was observed that, after the ultimate load an increase in the load capacity occurs due to strain hardening as shown below.

6. Comparison between fe results and design codes strength

The web crippling strengths from finite element analysis of pure web crippling models were compared with the nominal web crippling strengths calculated using Australian/New Zealand Standard AS/NZS 4600, Britain Standard BS 5950-5, Egyptian code ECP-LRFD and North American Specification NAS. Although NAS was not applicable for un-stiffened C-sections with inside bend radius to thickness ratios > 1.0, it was involved in the comparison to check the validity of using it for the studied range of parameters. In Tables 2–9, comparisons of the finite element strengths (P_{FE}) of the modeled channels with the nominal design strengths (P_n or P_w) are presented.

Figs. 13–16 show statistical comparison between the strength obtained from the finite element analysis, the strength estimated by the international codes of practice, and the experimentally predicted strength for the investigated channel series.

Based on the statistical analysis of the above tabulated results, the statistical criteria given in Table 10 can be estimated.

Table 2 Comparison of finite element web crippling strength P_{FE} with current design strengths for series S1.

Specimen label	Ratio				P_{FE} (kN)	Nominal web crippling strengths, P_n or P_w in kN				Comparisons, $P_{FE}/(P_n$ or $P_w)$			
	D/t	h/t	N/t	R/t		NAS	ECP	BS	AS/NZS	NAS	ECP	BS	AS/NZS
S1-C100×50N25	50.0	42.0	12.5	3.0	8.35	7.04	11.27	12.43	13.85	1.19	0.74	0.67	0.60
S1-C100×50N50	50.0	42.0	25.0	3.0	9.23	7.80	11.44	13.43	14.96	1.18	0.81	0.69	0.62
S1-C100×50N75	50.0	42.0	37.5	3.0	9.95	8.39	11.61	14.43	16.08	1.19	0.86	0.69	0.62
S1-C150×50N25	75.0	67.0	12.5	3.0	8.32	6.91	10.86	11.97	13.34	1.20	0.77	0.69	0.62
S1-C150×50N50	75.0	67.0	25.0	3.0	9.19	7.66	11.02	12.93	14.42	1.20	0.83	0.71	0.64
S1-C150×50N75	75.0	67.0	37.5	3.0	9.94	8.24	11.18	13.89	15.49	1.21	0.89	0.72	0.64
S1-C200×50N25	100.0	92.0	12.5	3.0	8.23	6.81	10.45	11.51	12.84	1.21	0.79	0.72	0.64
S1-C200×50N50	100.0	92.0	25.0	3.0	9.06	7.54	10.61	12.44	13.87	1.20	0.85	0.73	0.65
S1-C200×50N75	100.0	92.0	37.5	3.0	9.71	8.11	10.76	13.36	14.91	1.20	0.90	0.73	0.65
S1-C250×50N25	125.0	117.0	12.5	3.0	8.22	6.72	10.04	11.05	12.33	1.22	0.82	0.74	0.67
S1-C250×50N50	125.0	117.0	25.0	3.0	9.02	7.44	10.19	11.94	13.33	1.21	0.88	0.75	0.68
S1-C250×50N75	125.0	117.0	37.5	3.0	9.67	8.00	10.34	12.83	14.32	1.21	0.94	0.75	0.68

Table 3 Comparison of Finite Element Web Crippling strength P_{FE} with Current design strengths for series S2.

Specimen label	Ratio				P_{FE} kN	Nominal Web Crippling Strengths, P_n or P_w in kN				Comparisons, $P_{FE}/(P_n$ or $P_w)$			
	D/t	h/t	N/t	R/t		NAS	ECP	BS	AS/NZS	NAS	ECP	BS	AS/NZS
S2-C100×50N25	33.3	27.3	8.3	2.0	16.35	18.77	27.54	29.78	33.09	0.87	0.59	0.55	0.49
S2-C100×50N50	33.3	27.3	16.7	2.0	18.14	20.52	27.81	31.42	34.91	0.88	0.65	0.58	0.52
S2-C100×50N75	33.3	27.3	25.0	2.0	19.59	21.85	28.08	33.06	36.74	0.90	0.70	0.59	0.53
S2-C150×50N25	50.0	44.0	8.3	2.0	16.35	18.50	26.88	29.06	32.30	0.88	0.61	0.56	0.51
S2-C150×50N50	50.0	44.0	16.7	2.0	18.14	20.21	27.15	30.67	34.08	0.90	0.67	0.59	0.53
S2-C150×50N75	50.0	44.0	25.0	2.0	19.55	21.53	27.42	32.27	35.86	0.91	0.71	0.61	0.55
S2-C200×50N25	66.7	60.7	8.3	2.0	16.29	18.27	26.23	28.35	31.51	0.89	0.62	0.57	0.52
S2-C200×50N50	66.7	60.7	16.7	2.0	18.12	19.96	26.49	29.91	33.25	0.91	0.68	0.61	0.54
S2-C200×50N75	66.7	60.7	25.0	2.0	19.44	21.26	26.75	31.48	34.99	0.91	0.73	0.62	0.56
S2-C250×50N25	83.3	77.3	8.3	2.0	16.29	18.07	25.57	27.64	30.72	0.90	0.64	0.59	0.53
S2-C250×50N50	83.3	77.3	16.7	2.0	18.11	19.74	25.83	29.16	32.42	0.92	0.70	0.62	0.56
S2-C250×50N75	83.3	77.3	25.0	2.0	19.36	21.03	26.08	30.68	34.11	0.92	0.74	0.63	0.57

Table 4 Comparison of finite element web crippling strength P_{FE} with current design strengths for series S3.

Specimen label	Ratio				P_{FE} (kN)	Nominal web crippling strengths, P_n or P_w in kN				Comparisons, $P_{FE}/(P_n$ or $P_w)$			
	D/t	h/t	N/t	R/t		NAS	ECP	BS	AS/NZS	NAS	ECP	BS	AS/NZS
S3-C100×50N25	50.0	39.0	12.5	4.5	8.21	5.09	10.17	11.16	12.49	1.61	0.81	0.74	0.66
S3-C100×50N50	50.0	39.0	25.0	4.5	9.07	5.64	10.32	12.05	13.49	1.61	0.88	0.75	0.67
S3-C100×50N75	50.0	39.0	37.5	4.5	9.71	6.06	10.47	12.95	14.50	1.60	0.93	0.75	0.67
S3-C150×50N25	75.0	64.0	12.5	4.5	8.11	4.99	9.80	10.74	12.03	1.63	0.83	0.76	0.67
S3-C150×50N50	75.0	64.0	25.0	4.5	8.94	5.53	9.94	11.61	13.00	1.62	0.90	0.77	0.69
S3-C150×50N75	75.0	64.0	37.5	4.5	9.57	5.95	10.09	12.47	13.97	1.61	0.95	0.77	0.69
S3-C200×50N25	100.0	89.0	12.5	4.5	8.02	4.91	9.43	10.33	11.58	1.63	0.85	0.78	0.69
S3-C200×50N50	100.0	89.0	25.0	4.5	8.86	5.45	9.57	11.16	12.51	1.63	0.93	0.79	0.71
S3-C200×50N75	100.0	89.0	37.5	4.5	9.48	5.85	9.71	12.00	13.44	1.62	0.98	0.79	0.71
S3-C250×50N25	125.0	114.0	12.5	4.5	7.90	4.85	9.06	9.92	11.13	1.63	0.87	0.80	0.71
S3-C250×50N50	125.0	114.0	25.0	4.5	8.69	5.37	9.19	10.72	12.02	1.62	0.95	0.81	0.72
S3-C250×50N75	125.0	114.0	37.5	4.5	9.21	5.77	9.33	11.52	12.92	1.60	0.99	0.80	0.71

Table 5 Comparison of finite element web crippling strength P_{FE} with current design strengths for series S4.

Specimen label	Ratio				P_{FE} (kN)	Nominal web crippling strengths, P_n or P_w in kN				Comparisons, $P_{FE}/(P_n$ or $P_w)$			
	D/t	h/t	N/t	R/t		NAS	ECP	BS	AS/NZS	NAS	ECP	BS	AS/NZS
S4-C100×50N25	33.3	25.3	8.3	3.0	16.03	15.32	25.85	27.88	31.06	1.05	0.62	0.57	0.52
S4-C100×50N50	33.3	25.3	16.7	3.0	17.91	16.74	26.11	29.41	32.78	1.07	0.69	0.61	0.55
S4-C100×50N75	33.3	25.3	25.0	3.0	19.32	17.83	26.37	30.95	34.49	1.08	0.73	0.62	0.56
S4-C150×50N25	50.0	42.0	8.3	3.0	15.83	15.08	25.24	27.21	30.33	1.05	0.63	0.58	0.52
S4-C150×50N50	50.0	42.0	16.7	3.0	17.68	16.48	25.49	28.71	32.00	1.07	0.69	0.62	0.55
S4-C150×50N75	50.0	42.0	25.0	3.0	19.24	17.56	25.74	30.21	33.67	1.10	0.75	0.64	0.57
S4-C200×50N25	66.7	58.7	8.3	3.0	15.74	14.89	24.63	26.54	29.59	1.06	0.64	0.59	0.53
S4-C200×50N50	66.7	58.7	16.7	3.0	17.62	16.28	24.87	28.00	31.22	1.08	0.71	0.63	0.56
S4-C200×50N75	66.7	58.7	25.0	3.0	18.97	17.34	25.12	29.47	32.85	1.09	0.76	0.64	0.58
S4-C250×50N25	83.3	75.3	8.3	3.0	15.71	14.73	24.02	25.87	28.85	1.07	0.65	0.61	0.54
S4-C250×50N50	83.3	75.3	16.7	3.0	17.55	16.10	24.25	27.30	30.44	1.09	0.72	0.64	0.58
S4-C250×50N75	83.3	75.3	25.0	3.0	18.90	17.15	24.49	28.72	32.03	1.10	0.77	0.66	0.59

Table 6 Comparison of finite element web crippling strength P_{FE} with current design strengths for series S5.

Specimen label	Ratio				P_{FE} (kN)	Nominal web crippling strengths, P_n or P_w in kN				Comparisons, $P_{FE}/(P_n$ or $P_w)$			
	D/t	h/t	N/t	R/t		NAS	ECP	BS	AS/NZS	NAS	ECP	BS	AS/NZS
S5-C100×50N25	50.0	42.0	12.5	3.0	11.94	10.56	14.84	16.46	18.36	1.13	0.80	0.73	0.65
S5-C100×50N50	50.0	42.0	25.0	3.0	13.23	11.71	15.06	17.78	19.84	1.13	0.88	0.74	0.67
S5-C100×50N75	50.0	42.0	37.5	3.0	14.32	12.58	15.28	19.10	21.31	1.14	0.94	0.75	0.67
S5-C150×50N25	75.0	67.0	12.5	3.0	11.78	10.37	14.30	15.85	17.69	1.14	0.82	0.74	0.67
S5-C150×50N50	75.0	67.0	25.0	3.0	13.06	11.49	14.51	17.12	19.11	1.14	0.90	0.76	0.68
S5-C150×50N75	75.0	67.0	37.5	3.0	14.01	12.35	14.72	18.40	20.53	1.13	0.95	0.76	0.68
S5-C200×50N25	100.0	92.0	12.5	3.0	11.54	10.21	13.76	15.24	17.02	1.13	0.84	0.76	0.68
S5-C200×50N50	100.0	92.0	25.0	3.0	12.60	11.32	13.96	16.47	18.39	1.11	0.90	0.76	0.69
S5-C200×50N75	100.0	92.0	37.5	3.0	13.57	12.16	14.17	17.70	19.76	1.12	0.96	0.77	0.69
S5-C250×50N25	125.0	117.0	12.5	3.0	11.48	10.07	13.22	14.64	16.35	1.14	0.87	0.78	0.70
S5-C250×50N50	125.0	117.0	25.0	3.0	12.51	11.16	13.41	15.81	17.66	1.12	0.93	0.79	0.71
S5-C250×50N75	125.0	117.0	37.5	3.0	13.38	12.00	13.61	16.99	18.98	1.12	0.98	0.79	0.71

Table 7 Comparison of finite element web crippling strength P_{FE} with current design strengths for series S6.

Specimen label	Ratio				P_{FE} (kN)	Nominal web crippling strengths, P_n or P_w in kN				Comparisons, $P_{FE}/(P_n$ or $P_w)$			
	D/t	h/t	N/t	R/t		NAS	ECP	BS	AS/NZS	NAS	ECP	BS	AS/NZS
S6-C100×50N25	33.3	27.3	8.3	2.0	21.34	28.16	36.25	39.44	43.86	0.76	0.59	0.54	0.49
S6-C100×50N50	33.3	27.3	16.7	2.0	25.17	30.77	36.61	41.61	46.28	0.82	0.69	0.60	0.54
S6-C100×50N75	33.3	27.3	25.0	2.0	28.92	32.78	36.97	43.78	48.69	0.88	0.78	0.66	0.59
S6-C150×50N25	50.0	44.0	8.3	2.0	21.33	27.74	35.39	38.49	42.81	0.77	0.60	0.55	0.50
S6-C150×50N50	50.0	44.0	16.7	2.0	25.12	30.32	35.74	40.61	45.17	0.83	0.70	0.62	0.56
S6-C150×50N75	50.0	44.0	25.0	2.0	28.76	32.29	36.09	42.73	47.53	0.89	0.80	0.67	0.61
S6-C200×50N25	66.7	60.7	8.3	2.0	21.18	27.40	34.53	37.54	41.77	0.77	0.61	0.56	0.51
S6-C200×50N50	66.7	60.7	16.7	2.0	24.96	29.94	34.87	39.61	44.07	0.83	0.72	0.63	0.57
S6-C200×50N75	66.7	60.7	25.0	2.0	28.45	31.89	35.21	41.68	46.37	0.89	0.81	0.68	0.61
S6-C250×50N25	83.3	77.3	8.3	2.0	21.16	27.10	33.66	36.60	40.72	0.78	0.63	0.58	0.52
S6-C250×50N50	83.3	77.3	16.7	2.0	24.92	29.62	34.00	38.62	42.97	0.84	0.73	0.65	0.58
S6-C250×50N75	83.3	77.3	25.0	2.0	28.38	31.55	34.33	40.63	45.21	0.90	0.83	0.70	0.63

Table 8 Comparison of finite element web crippling strength P_{FE} with current design strengths for series S7.

Specimen label	Ratio				P_{FE} (kN)	Nominal web crippling strengths, P_n or P_w in kN				Comparisons, $P_{FE}/(P_n$ or $P_w)$			
	D/t	h/t	N/t	R/t		NAS	ECP	BS	AS/NZS	NAS	ECP	BS	AS/NZS
S7-C100×50N25	50.0	39.0	12.5	4.5	11.66	7.63	13.38	14.77	16.55	1.53	0.87	0.79	0.70
S7-C100×50N50	50.0	39.0	25.0	4.5	12.98	8.46	13.58	15.96	17.88	1.53	0.96	0.81	0.73
S7-C100×50N75	50.0	39.0	37.5	4.5	13.81	9.09	13.78	17.15	19.22	1.52	1.00	0.81	0.72
S7-C150×50N25	75.0	64.0	12.5	4.5	11.51	7.49	12.90	14.23	15.95	1.54	0.89	0.81	0.72
S7-C150×50N50	75.0	64.0	25.0	4.5	12.67	8.30	13.09	15.37	17.23	1.53	0.97	0.82	0.73
S7-C150×50N75	75.0	64.0	37.5	4.5	13.62	8.92	13.28	16.52	18.52	1.53	1.03	0.82	0.74
S7-C200×50N25	100.0	89.0	12.5	4.5	11.33	7.37	12.41	13.68	15.35	1.54	0.91	0.83	0.74
S7-C200×50N50	100.0	89.0	25.0	4.5	12.49	8.17	12.59	14.79	16.59	1.53	0.99	0.84	0.75
S7-C200×50N75	100.0	89.0	37.5	4.5	13.26	8.78	12.78	15.89	17.82	1.51	1.04	0.83	0.74
S7-C250×50N25	125.0	114.0	12.5	4.5	11.03	7.27	11.92	13.14	14.75	1.52	0.93	0.84	0.75
S7-C250×50N50	125.0	114.0	25.0	4.5	12.25	8.06	12.10	14.20	15.94	1.52	1.01	0.86	0.77
S7-C250×50N75	125.0	114.0	37.5	4.5	13.20	8.66	12.28	15.25	17.12	1.52	1.07	0.87	0.77

Table 9 Comparison of finite element web crippling strength PFE with current design strengths for series S8.

Specimen label	Ratio				P_{FE} (kN)	Nominal web crippling strengths, P_n or P_w in kN				Comparisons, $P_{FE}/(P_n$ or $P_w)$			
	D/t	h/t	N/t	R/t		NAS	ECP	BS	AS/NZS	NAS	ECP	BS	AS/NZS
S8-C100×50N25	33.3	25.3	8.3	3.0	20.45	22.98	34.03	36.92	41.18	0.89	0.60	0.55	0.50
S8-C100×50N50	33.3	25.3	16.7	3.0	24.14	25.11	34.37	38.95	43.45	0.96	0.70	0.62	0.56
S8-C100×50N75	33.3	25.3	25.0	3.0	27.22	26.74	34.71	40.99	45.72	1.02	0.78	0.66	0.60
S8-C150×50N25	50.0	42.0	8.3	3.0	20.44	22.63	33.23	36.03	40.20	0.90	0.62	0.57	0.51
S8-C150×50N50	50.0	42.0	16.7	3.0	24.14	24.73	33.56	38.02	42.41	0.98	0.72	0.63	0.57
S8-C150×50N75	50.0	42.0	25.0	3.0	27.20	26.34	33.88	40.01	44.63	1.03	0.80	0.68	0.61
S8-C200×50N25	66.7	58.7	8.3	3.0	20.34	22.34	32.42	35.15	39.22	0.91	0.63	0.58	0.52
S8-C200×50N50	66.7	58.7	16.7	3.0	23.84	24.41	32.74	37.08	41.38	0.98	0.73	0.64	0.58
S8-C200×50N75	66.7	58.7	25.0	3.0	27.11	26.01	33.06	39.02	43.54	1.04	0.82	0.69	0.62
S8-C250×50N25	83.3	75.3	8.3	3.0	20.24	22.09	31.61	34.26	38.24	0.92	0.64	0.59	0.53
S8-C250×50N50	83.3	75.3	16.7	3.0	23.61	24.14	31.93	36.15	40.35	0.98	0.74	0.65	0.59
S8-C250×50N75	83.3	75.3	25.0	3.0	26.94	25.72	32.24	38.04	42.46	1.05	0.84	0.71	0.63

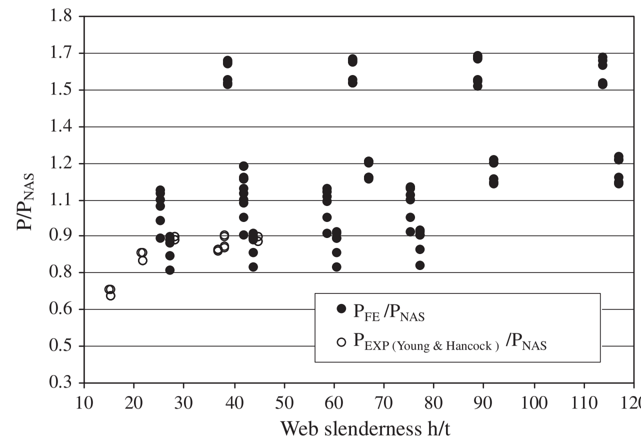

Figure 13 Finite element strength versus design strength of NAS.

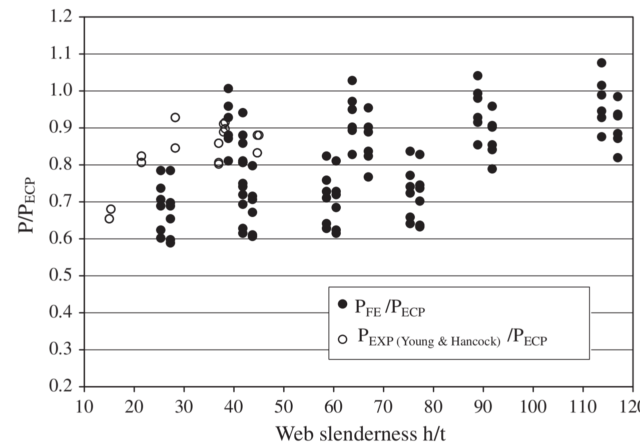

Figure 14 Finite element strength versus design strength of ECP.

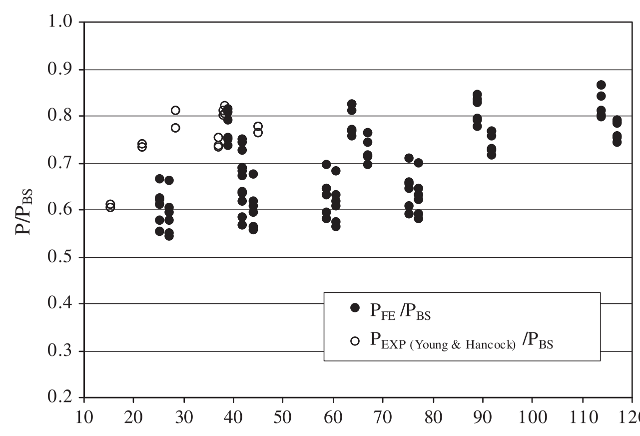

Figure 15 Finite element strength versus design strength of BS.

It is clear that all provisions are not adequate for predicting the web crippling strength as the values of reliability index are less than 2.5 as specified in NAS for members design.

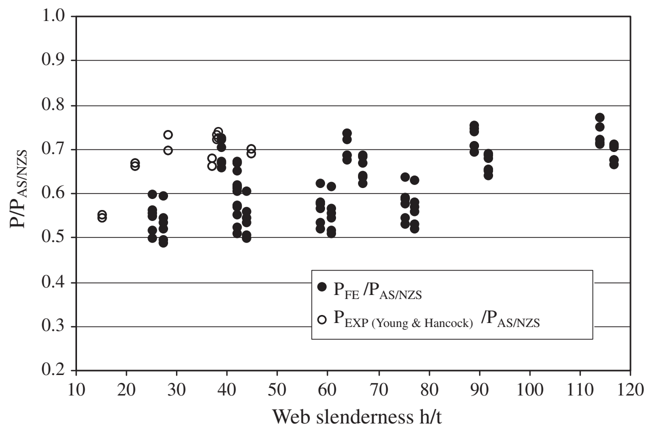

Figure 16 Finite element strength versus design strength of AS/NZS.

Table 10 Statistical parameters for the different codes of practice.

Item	NAS	ECP	BS	AS/NZS
Mean value of $P_{FE}/(P_n$ or $P_w)$	1.16	0.81	0.70	0.63
Coefficient of variation	0.253	0.147	0.124	0.123
Reliability index (β)	2.18	1.64	1.20	0.80

7. Proposed web crippling coefficients

In this section, new coefficients are proposed for the web crippling design equations of ECP and NAS specifications. The new coefficients are proposed to improve the prediction of web crippling strength for un-stiffened C-sections subjected to IOF loading and unfastened through their flanges. The proposed coefficients are based on statistical analysis of 24 test data points from literature [12] in addition to the finite element analysis results of 96 web crippling models investigated in this research. The following proposed coefficients were obtained after several trials with different coefficient values to minimize the coefficient of variation.

7.1. Proposed coefficients for ECP

Table 11a shows a comparison between the original coefficients adopted by the ECP and the proposed coefficients for the web crippling resistance for shapes having single thickness webs subjected to IOF loading:

7.2. Proposed coefficients for NAS

Table 11b shows a comparison between the original coefficients adopted by the NAS and the proposed coefficients for the web crippling strength of single web C-sections subjected to IOF loading:

Table 11b Current and proposed coefficients of the NAS design equation.

Coefficients	C	C_R	C_N	C_h
Current value	13	0.32	0.10	0.010
Proposed value	6.5	0.15	0.15	0.001

Table 12 Statistical parameters for the modified ECP and NAS coefficients.

Item	NAS modified	ECP modified
Mean value of $P_{FE}/(P_n$ or $P_w)$	1.10	1.09
Coefficient of variation	0.09	0.10
Reliability index (β)	2.96	2.95

Table 12 shows the statistical parameters for the ECP and NAS after adopting the coefficients listed in Tables 11a and 11b respectively.

As can be noticed from Table 12, the values of reliability index (β) for the modified coefficients are larger than 2.5, which is complying with the NAS requirements. Comparing the statistical parameters shown in Table 10 to those show in Table 12, it can be concluded that the proposed coefficients considerably improve the statistical parameters of the two design codes.

8. Combined bending and web crippling

Tables 13–16 present the analysis results of combined bending and web crippling finite element models. In tables, three values of finite element loads were presented with their corresponding bending moments for each modeled channel. The first value $P_{C\text{-}FE}$ was obtained from pure web crippling model while the other two values were obtained from interaction models for spans 1000 and 2000 mm respectively. The corresponding moments $M_{C\text{-}FE}$ were simply calculated as the load times the span divided by 4.

Figs. 17 and 18 show samples of von misses stress distribution and deformed shapes for different interaction bending and web crippling models at the ultimate load. It has been observed in all models with channel depths greater than 100 mm and having 1000 mm span length that, yielding first occurs at the top web–flange intersection along the bearing load length. On the other hand, for most models having 2000 mm span length, yielding first occurs at the bottom web–flange intersection due to lateral buckling of bottom flanges as shown in Figs. 17 and 18.

Fig. 19 shows the load versus web deformation for two different interaction bending and web crippling models. It

Table 11a Current and proposed coefficients of the ECP design equation.

Coefficients	C_1	C_2	C_{15}	C_{19}
Current value	$1.22–0.100F_y$	$1.06–0.06(R/t)$	$3350–4.60(h/t)$	$1 + 0.0012(N/t)$
Proposed value	$1.15–0.001F_y$	$1.05–0.05(R/t)$	$1300–0.05(h/t)$	$1 + 0.0200(N/t)$

Table 13 Finite element results of combined bending and web crippling for series S5.

Specimen label	Web crippling		Span $L = 1000$ mm		Span $L = 2000$ mm	
	P_{FE} (kN)	M_{FE} (kN m)	$P_{C\text{-}FE}$ (kN)	$M_{C\text{-}FE}$ (kN m)	$P_{C\text{-}FE}$ (kN)	$M_{C\text{-}FE}$ (kN m)
S5-C100×50×2-R6-N25	10.45	1.08	8.05	2.01	5.80	2.90
S5-C100×50×2-R6-N50	12.24	1.35	9.68	2.42	6.65	3.32
S5-C100×50×2-R6-N75	13.62	1.58	10.82	2.71	6.84	3.42
S5-C150×50×2-R6-N25	10.26	1.45	10.43	2.61	7.72	3.86
S5-C150×50×2-R6-N50	12.02	1.77	11.46	2.87	8.62	4.31
S5-C150×50×2-R6-N75	13.37	2.06	12.43	3.11	9.67	4.84
S5-C200×50×2-R6-N25	10.10	1.81	11.01	2.75	8.98	4.49
S5-C200×50×2-R6-N50	11.83	2.19	12.02	3.00	9.88	4.94
S5-C200×50×2-R6-N75	13.16	2.52	13.00	3.25	10.59	5.30
S5-C250×50×2-R6-N25	9.96	2.15	11.30	2.82	9.85	4.92
S5-C250×50×2-R6-N50	11.67	2.60	12.38	3.10	10.74	5.37
S5-C250×50×2-R6-N75	12.99	2.97	13.22	3.31	11.49	5.74

Table 14 Finite element results of combined bending and web crippling for series S6.

Specimen label	Web crippling		Span $L = 1000$ mm		Span $L = 2000$ mm	
	P_{FE} (kN)	M_{FE} (kN m)	$P_{C\text{-}FE}$ (kN)	$M_{C\text{-}FE}$ (kN m)	$P_{C\text{-}FE}$ (kN)	$M_{C\text{-}FE}$ (kN m)
S6-C100×50×3-R6-N25	21.34	2.21	17.07	4.27	10.07	5.03
S6-C100×50×3-R6-N50	25.17	2.77	17.35	4.34	12.96	6.48
S6-C100×50×3-R6-N75	28.92	3.36	22.34	5.58	13.01	6.50
S6-C150×50×3-R6-N25	21.33	3.01	20.17	5.04	16.44	8.22
S6-C150×50×3-R6-N50	25.12	3.71	22.47	5.62	17.36	8.68
S6-C150×50×3-R6-N75	28.76	4.42	24.88	6.22	17.08	8.54
S6-C200×50×3-R6-N25	21.18	3.79	21.29	5.32	17.54	8.77
S6-C200×50×3-R6-N50	24.96	4.62	24.25	6.06	19.42	9.71
S6-C200×50×3-R6-N75	28.45	5.44	26.16	6.54	19.89	9.94
S6-C250×50×3-R6-N25	21.16	4.58	22.35	5.59	19.34	9.67
S6-C250×50×3-R6-N50	24.92	5.55	25.30	6.33	21.34	10.67
S6-C250×50×3-R6-N75	28.38	6.49	27.15	6.79	23.11	11.55

Table 15 Finite element results of combined bending and web crippling for series S7.

Specimen label	Web crippling		Span $L = 1000$ mm		Span $L = 2000$ mm	
	P_{FE} (kN)	M_{FE} (kN m)	$P_{C\text{-}FE}$ (kN)	$M_{C\text{-}FE}$ (kN m)	$P_{C\text{-}FE}$ (kN)	$M_{C\text{-}FE}$ (kN m)
S7-C100×50×2-R9-N25	12.04	1.25	7.62	1.90	5.36	2.68
S7-C100×50×2-R9-N50	12.98	1.43	8.73	2.18	6.10	3.05
S7-C100×50×2-R9-N75	13.81	1.61	9.78	2.44	6.33	3.16
S7-C150×50×2-R9-N25	11.51	1.63	10.11	2.53	7.38	3.69
S7-C150×50×2-R9-N50	12.67	1.87	11.39	2.85	8.03	4.01
S7-C150×50×2-R9-N75	13.62	2.09	11.95	2.99	8.74	4.37
S7-C200×50×2-R9-N25	11.33	2.03	10.77	2.69	8.95	4.47
S7-C200×50×2-R9-N50	12.49	2.31	11.99	3.00	9.85	4.93
S7-C200×50×2-R9-N75	13.26	2.54	12.63	3.16	10.41	5.20
S7-C250×50×2-R9-N25	11.03	2.39	10.83	2.71	9.65	4.82
S7-C250×50×2-R9-N50	12.25	2.73	12.08	3.02	11.49	5.74
S7-C250×50×2-R9-N75	13.20	3.02	12.66	3.17	10.98	5.49

was observed in some models that, an increase in the load capacity occurred after the ultimate load due to strain hardening.

All codes of practice adopt interaction equations to account for the interaction between bending and web crippling. Fig. 20 shows comparisons between the interaction strength obtained from the finite element analysis, and those obtained from AS/NZS, BS, and ECP/NAS interaction equations. Codes results shown at these figures are based on the original equations before introducing the proposed modifications presented at the previous section.

As can be noticed from Figs. 20a–20d, the AS/NZS, BS and ECP codes generally overestimate the interactive strength, while the results obtained by the NAS codes are generally conservative. Accordingly, it is recommended to utilize the modified web crippling formulae given by Tables 11a and 11b.

Table 16 Finite element results of combined bending and web crippling for series S8.

Specimen label	Web crippling		Span L = 1000 mm		Span L = 2000 mm	
	P_{FE} (kN)	M_{FE} (kN m)	$P_{C\text{-}FE}$ (kN)	$M_{C\text{-}FE}$ (kN m)	$P_{C\text{-}FE}$ (kN)	$M_{C\text{-}FE}$ (kN m)
S8-C100×50×3-R9-N25	20.45	2.12	15.20	3.80	11.34	5.67
S8-C100×50×3-R9-N50	24.14	2.66	17.35	4.34	12.13	6.07
S8-C100×50×3-R9-N75	27.22	3.16	17.91	4.48	10.70	5.35
S8-C150×50×3-R9-N25	20.44	2.89	19.08	4.77	13.75	6.88
S8-C150×50×3-R9-N50	24.14	3.56	21.16	5.29	18.44	9.22
S8-C150×50×3-R9-N75	27.20	4.18	18.64	4.66	18.64	9.32
S8-C200×50×3-R9-N25	20.34	3.64	20.41	5.10	16.71	8.36
S8-C200×50×3-R9-N50	23.84	4.41	23.73	5.93	21.19	10.60
S8-C200×50×3-R9-N75	27.11	5.18	25.38	6.35	19.05	9.53
S8-C250×50×3-R9-N25	20.24	4.38	21.44	5.36	18.68	9.34
S8-C250×50×3-R9-N50	23.61	5.25	24.48	6.12	20.56	10.28
S8-C250×50×3-R9-N75	26.94	6.16	26.02	6.50	21.79	10.90

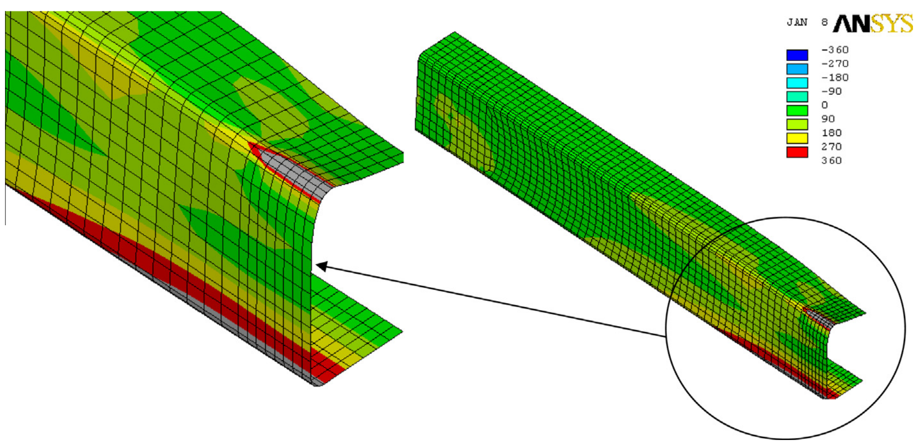

Figure 17 Von Mises stress of model S5-C100×50×2-R6-N75-F360-L109.

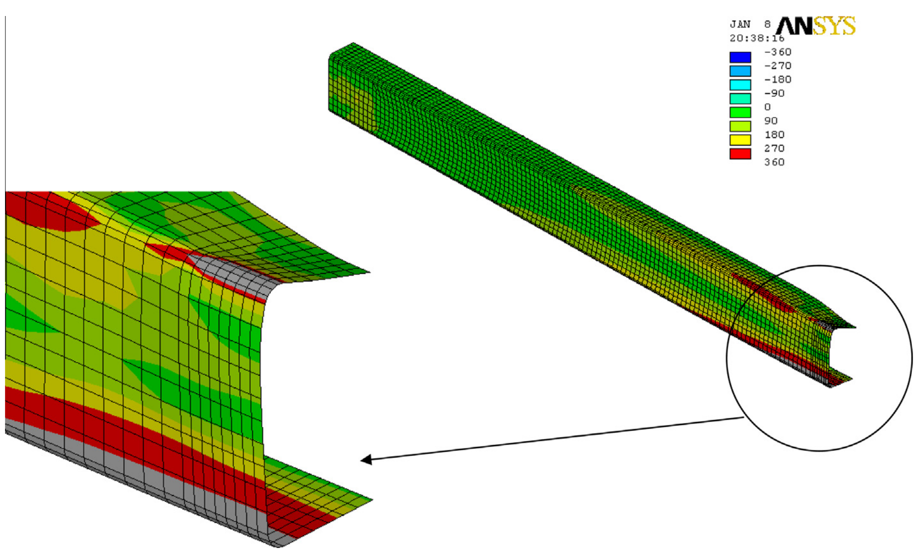

Figure 18 Von Mises stress of model S5-C100×50×2-R6-N75-F360-L209.

Utilizing the modified coefficients, results in the comparison shown in Figs. 21a and 21b.

Fig. 21a declares that, utilizing the proposed web crippling coefficients given by Table 11a is important to improve the results of the ECP-interaction. On the other hand, the effect of utilizing the proposed coefficients given by Table 11b on the interaction equations given by NAS is insignificant as show in Fig. 21b.

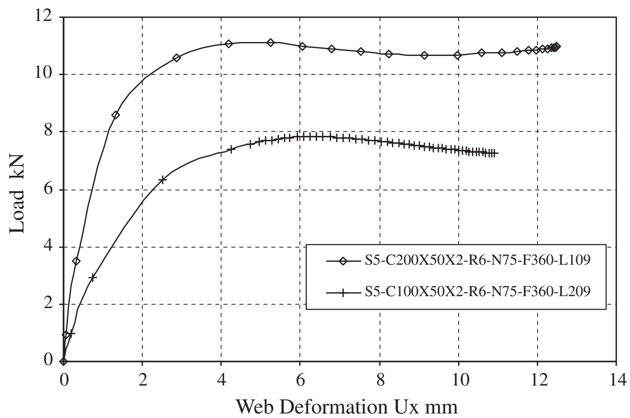

Figure 19 Load versus web deformation of interaction models "S5-C200×50×2-R6-N75-F360".

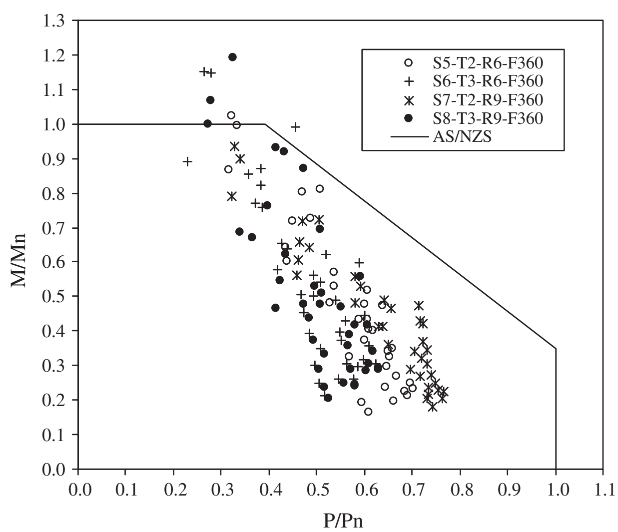

Figure 20a Finite element results versus AS/NZS-interaction design equation.

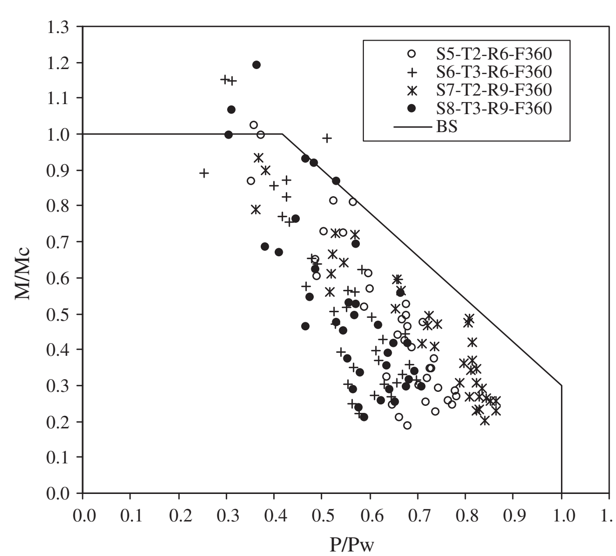

Figure 20b Finite element results versus BS-interaction design equation.

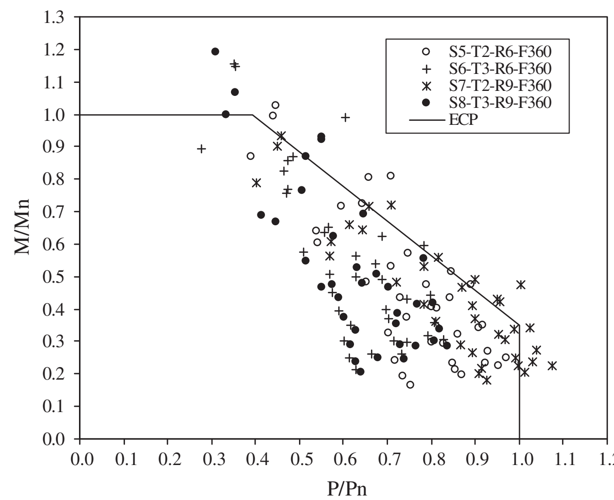

Figure 20c Finite element results versus ECP-interaction design equations.

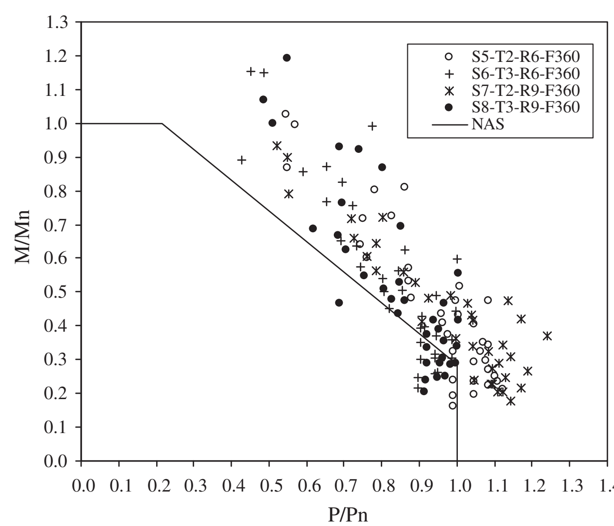

Figure 20d Finite element results versus NAS-interaction design equations.

9. Conclusion

Based on the results of the parametric study on cold formed steel channels subjected to web crippling and combined bending and web crippling under IOF loading conditions, the following concluding remarks can be drawn:

(1) Results of the finite element model developed to investigate the web crippling and web crippling combined with bending were found to be in a good agreement with the experimental results available in literatures.
(2) Both AS/NZS and BS standards were found to be generally inadequate for estimating the web crippling strengths of the studied range of cold formed steel channels under IOF loading.

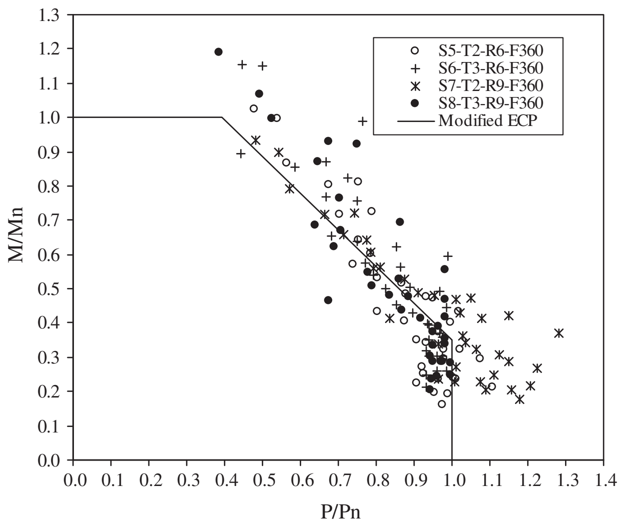

Figure 21a Finite element results versus modified ECP-interaction equations.

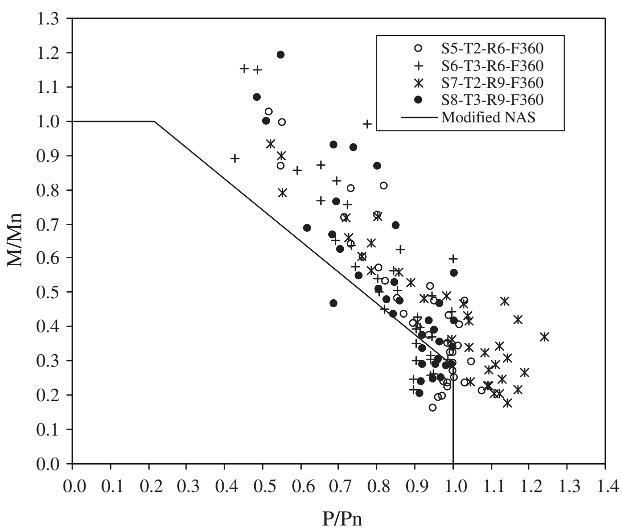

Figure 21b Finite element results versus modified NAS-interaction equations.

(3) The predicted web crippling strength using NAS was acceptable for 53% of the studied cases while the predicted strengths using ECP was acceptable only for 4%.
(4) The proposed coefficient enhanced the predicted web crippling strength using ECP code. The improved strength became acceptable for 73% of tested sections.
(5) The predicted web crippling strength using NAS with the proposed coefficients has improved and became acceptable for 80% of investigated cases.
(6) The interaction design equations in both AS/NZS and BS standards are generally inadequate for the studied range of parameters.
(7) The interaction design equations in both ECP and NAS are adequate for the studied range of parameters.

References

[1] ANSYS 5.4. "User's Manual", Swanson Analysis System, USA; 1999.
[2] Australian/New Zealand standard (AS/NZS 4600). "Cold-formed steel structures", Sydney, Australia; 1996.
[3] Beshara B. Web crippling of cold-formed steel members, M. A. Sc. Thesis, University of Waterloo, Waterloo, Canada; 1999.
[4] Beshara B, Schuster R. Web crippling data and calibrations of cold formed steel members, final report, University of Waterloo, Waterloo, Ontario, Canada; 2000.
[5] British Standards Institution (BS 5950). Structural use of steelwork in building: Part 5, Code of practice for design of cold formed sections, London, UK; 1998.
[6] Egyptian Code of Practice for Steel Construction (ECP-LRFD). Load and Resistance Factor Design, (205) Ministerial Decree No 359. Cairo, Egypt; 2007.
[7] Kaitila O. Web crippling of cold-formed thin-walled steel cassettes, PhD Thesis, Helsinki University, Finland; 2004.
[8] North American Specification (NAS). Specification for the design of cold-formed steel structural members, Washington, DC; 2007.
[9] Prabakaran K. Web crippling of cold formed steel sections, M. A. Sc. thesis, University of Waterloo, Waterloo, Ontario, Canada; 1993.
[10] Ren WX et al.. Analysis and design of cold-formed steel channels subjected to combined bending and web crippling. Thin-Walled Struct 2006;44(5):314–20.
[11] Ren WX et al.. Finite-element simulation and design of cold-formed steel channels subjected to web crippling. J Struct Eng ASCE 2006;132(12):1967–75.
[12] Young B, Hancock G. Design of cold-formed channels subjected to web crippling. J Struct Eng ASCE 2001;127(10):1137–44.
[13] Young B, Hancock G. Tests of channels subjected to combined bending and web crippling. J Struct Eng ASCE 2002;128(3):300–8.
[14] Young B, Hancock G. Web crippling of cold-formed un-lipped channels with flanges restrained. Thin-Walled Struct 2004;42:911–30.
[15] Young B, Hancock G. Web crippling behavior of cold-formed steel sections with single web. Steel Struct 2005;5:79–85.
[16] Yu WW. Cold formed steel design. 3rd ed. New York: Wiley; 2000.

Mohamed S. Soliman is an associate professor of steel structures, at the faculty of engineering, Shobra, Benha University. He lectures design and behavior of steel structures and bridges. His research interests include steel construction and behavior of steel elements

Anwar B. Badawy Abu-Sena is an associate professor of steel structures, at the faculty of engineering, Shobra, Benha University. He lectures Design and Behavior of steel structures. His research interest is structural behavior of Steel elements.

Emad E. H. Darwish is a lecturer of steel structures, at the faculty of engineering, Shobra, Benha University. He lectures Design and Behavior of steel structures. His research interest is structural behavior of steel elements.

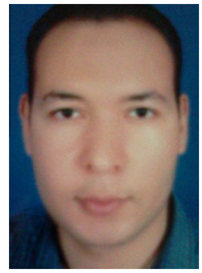

Mohamed S. R. Saleh is an assistant lecturer of structural engineering at the faculty of engineering, Shobra, Benha University. His research interest is structural behavior of steel elements.